

hydrodynamic torque due to the imposed shear flow field. At $k_2 = 0$, Jeffery's results are reproduced and all solutions of the equations starting from different initial conditions tend towards a fixed point in the stroboscopic plot.

Chapter 3

Chaotic Dynamics with a Potential Application to Particle Separation

3.1 Introduction

In the previous chapter, we described the formulation of a set of equations governing the dynamics of periodically forced spheroids in simple shear flow based on a model given by Brenner (1974). The control parameters that can be varied in equations 2.18 and 2.21 are k_1, k_2, k_3, ω and r_e . The evolution can be simulated in a computer for different values of these control parameters. In what follows we vary one of the control parameters in 2.21 by keeping the others constant for a systematic simulation. A number of chaotic regimes have been established by the simulation for these parameters.

3.2 Existence of chaotic regimes

As a first step in analyzing the properties of the equations derived in this work, we set $k_1 = k_3 = 0$ and varied k_2 between 0.0 and 20.0 for $r_e = 1.6$ and between 0.0 and 100.0 for $r_e = 0.4$ and kept ω equal to J . We expect the greatest complexity of the solutions of these equations for this particular choice of parameters, since k_2 is responsible for the greatest opposition to the

hydrodynamic torque due to the imposed shear flow field. At $k_2 = 0$, Jeffery's results are reproduced and all solutions of the equations starting from different initial conditions tend towards a fixed point in the stroboscopic plot.

We ran the program for 2500 points of the Poincaré section (stroboscopic plot) and deleted the first 2250 points to remove the transients. All runs were started with the initial conditions $\theta = \phi = 45^\circ$. For each trajectory we evaluated 100 points in each cycle which resulted in 25000 points of the trajectory after the transients are removed. We obtained identical results when ϕ was replaced by $-\phi$. As a test case when we ran the program for $\theta = 90^\circ$ the trajectory plot reduced to a continuous curve, indicating regular behaviour for all the values of k_2 considered. At $k_2 = 0.03$ for $r_e = 1.6$, the attractor slowly begins to broaden from a continuous curve and the Lyapunov exponent first becomes positive. There are a number of regular regimes in between the chaotic regimes. In our system, chaos usually appears as a broadening of the attractor as can be seen from the example given in Fig. 3.1. In certain regimes as in Ramamohan *et al.*, (1994) the attractor broadens to such an extent that a subset of the phase space is completely filled. Ramamohan *et al.* (1994) have analyzed the orientational dynamics of periodically forced slender rigid rods in simple shear flow under the action of a sinusoidal driver. Our equation 2.21 reduces to equations 2.6, 2.8 and 2.9 of Ramamohan *et al.* (1994) after suitable scaling and letting r_e tend to ∞ . Ramamohan *et al.* (1994) also kept $k_1 = k_3 = 0$ and varied k_2 between 0 and 1 ω was kept equal to 1 in Ramamohan (*et al.*, 1994). In Ramamohan (*et al.*, 1994) at $k_2 = 0.005$ the attractor slowly begin to broaden compared to $k_2 = 0.03$ for $r_e = 1.6$ in this work. Ramamohan *et al.* (1994) observed transient chaos at $k_2 = 0.25$. However for $r_e = 1.6$ we first obtained transient chaos at $k_2 = 4.5$. In this work we have tentatively identified chaotic regimes of the parameter k_2 namely for $r_e = 1.6$. Based on a similar analysis we obtained a chaotic regime for $r_e = 0.4$.

One paper resulting from this work has been accepted for presentation in an international conference, ICTAM held in JAPAN, 1996.

3.3 Results on separation technique

During our computations, we noted that the results of the computations are very sensitive to the aspect ratio of the particle in some parameter regimes as given in Fig. 3.2 for $\omega = J$. In the case of constant external fields (*i. e.* $\omega = 0$) in the same parametric regimes we obtained regular behaviour. For $r_e > 1.0$, we obtained nearly the same fixed point in the Poincaré section for all initial conditions in the case of a constant force field. This suggested the possibility of separating particles based on this observation.

To develop quantitative results based on this observation, we divided the range of possible orientations namely $[-90^\circ, 90^\circ]$ in both θ and ϕ variables into 7 equal intervals resulting in 49 equal sized grids. We then computed the evolution of initially uniformly distributed particles of different aspect ratio within the range of r_e equal to 0.2 to 2 in steps of 0.2. We followed the evolution of the initially uniformly distributed particles within the above range of particle axis ratios under the effect of constant, periodic and zero force fields. We followed the evolution of the ensemble of particles from 3001 to 5000 points of the Poincaré section in the case of periodic, constant and zero forces. In all cases we calculated the number of particles in each grid on every 4th iteration of the Poincaré section of the evolution equations resulting in a total of 500 values for periodic, constant and zero forces. We noted the grids in which the total number of particles was greater than or equal to 5 and also noted the number of particles in each grid only if the particle occurred in that grid in more than 10 iterations in all the cases. We denote these values as r_e, l_1 and l_2 , where r_e, l_1 and l_2 denote the aspect ratio, total number of occurrences of the grid and total number of particles in the grid on the average respectively and

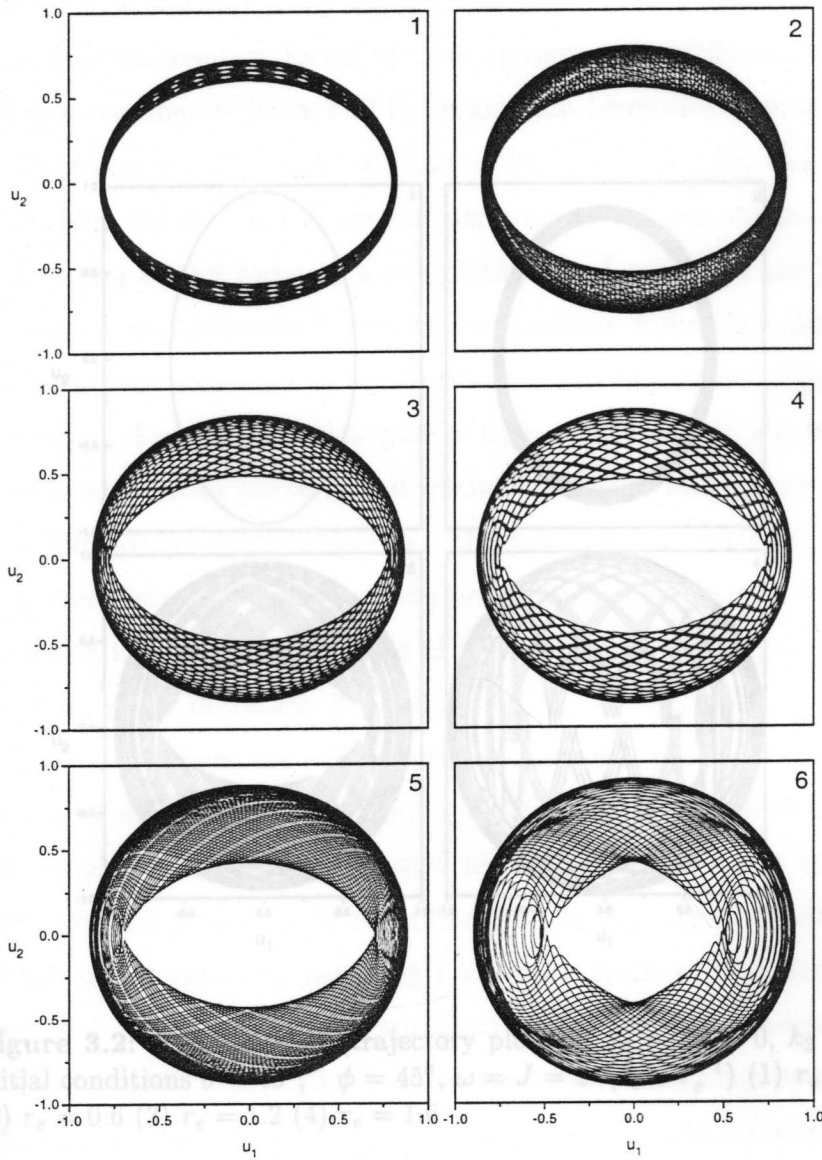


Figure 3.1: The trajectory plot of u_1 vs. u_2 for initial conditions $\theta = 45^\circ$, $\phi = 45^\circ$, $\omega = J = 2\pi(r_e + r_e^{-1})$, $r_e = 1.6$ and (1) $k_2=1.0$ (2) $k_2=2.0$ (3) $k_2=3.0$ (4) $k_2=3.5$ (5) $k_2=4.0$ (6) $k_2=4.5$.

prepared tables for these values. Since our preliminary computations indicated the greatest sensitivity of the results to the aspect ratio at $k_2 = 10$, we ran the program for k_2 equal to 9.5, 10 and 10.5 for periodic and constant forces.

In the case of constant forces, all the attractors for different aspect ratios resulted in a continuous curve and the maximum Lyapunov exponent was zero for all initial conditions, indicating regular behavior. Similar results were obtained for zero forces. In the case of periodic forces the attractors resulted in a broadening of the torus or a completely filled subset of the phase space and the maximum Lyapunov exponent was positive, indicating chaotic behavior. The Lyapunov exponent of the time series was calculated using the Kantz (1994) method. For aspect ratios greater than or equal to 1.0, all the attractors reduce to a continuous curve for all initial conditions and forces $k_2 = 9.5, 10$

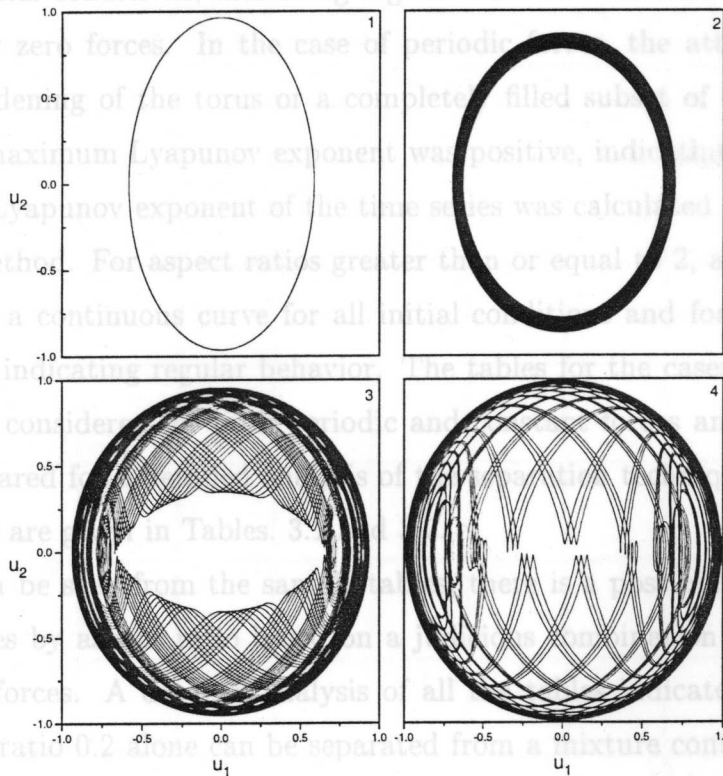


Figure 3.2: The attractor (trajectory plot) for $k_1 = k_3 = 0$, $k_2 = 10$, initial conditions $\theta = 45^\circ$, $\phi = 45^\circ$, $\omega = J = 2\pi(r_e + r_e^{-1})$ (1) $r_e = 0.2$ (2) $r_e = 0.6$ (3) $r_e = 1.2$ (4) $r_e = 1.6$

prepared tables for these values. Since our preliminary computations indicated the greatest sensitivity of the results to the aspect ratio at $k_2 = 10$, we ran the program for k_2 equal to 9.5, 10 and 10.5 for periodic and constant forces.

In the case of constant forces, all the attractors for different aspect ratios resulted in a continuous curve and the maximum Lyapunov exponent was zero for all initial conditions, indicating regular behavior. Similar results were obtained for zero forces. In the case of periodic forces, the attractors resulted in a broadening of the torus or a completely filled subset of the phase space and the maximum Lyapunov exponent was positive, indicating chaotic behavior. The Lyapunov exponent of the time series was calculated using the Kantz (1994) method. For aspect ratios greater than or equal to 2, all the attractors reduce to a continuous curve for all initial conditions and forces $k_2 = 9.5, 10$ and 10.5, indicating regular behavior. The tables for the cases of $k_2 = 9.5, 10$ and 10.5, considered for both periodic and constant forces and for zero force were prepared for a detailed analysis of the separation technique. A sample of the tables are given in Tables. 3.1 and 3.2.

As can be seen from the sample tables, there is a possibility of separation of particles by aspect ratio based on a judicious combination of periodic and constant forces. A detailed analysis of all the tables indicates that particles of aspect ratio 0.2 alone can be separated from a mixture containing particles of different aspect ratios by applying a constant force $k_2 = 0$, since particles of aspect ratio 0.2 alone occur on some extreme grids on the boundary of the tables. This suggests that particles of this aspect ratio alone can be separated by applying a zero force. In the case of particles of aspect ratio 0.4 a constant force between 9.5 and 10.5 appears to be sufficient for separating these particles alone. For separating particles of aspect ratio 0.6, it is desirable to apply a constant force between 9.5 and 10.5. Here particles of this aspect ratio alone occur in the centre grids for constant forces. Based on a similar analysis, periodic forces leading to chaotic dynamics or constant forces leading to regular dynamics of

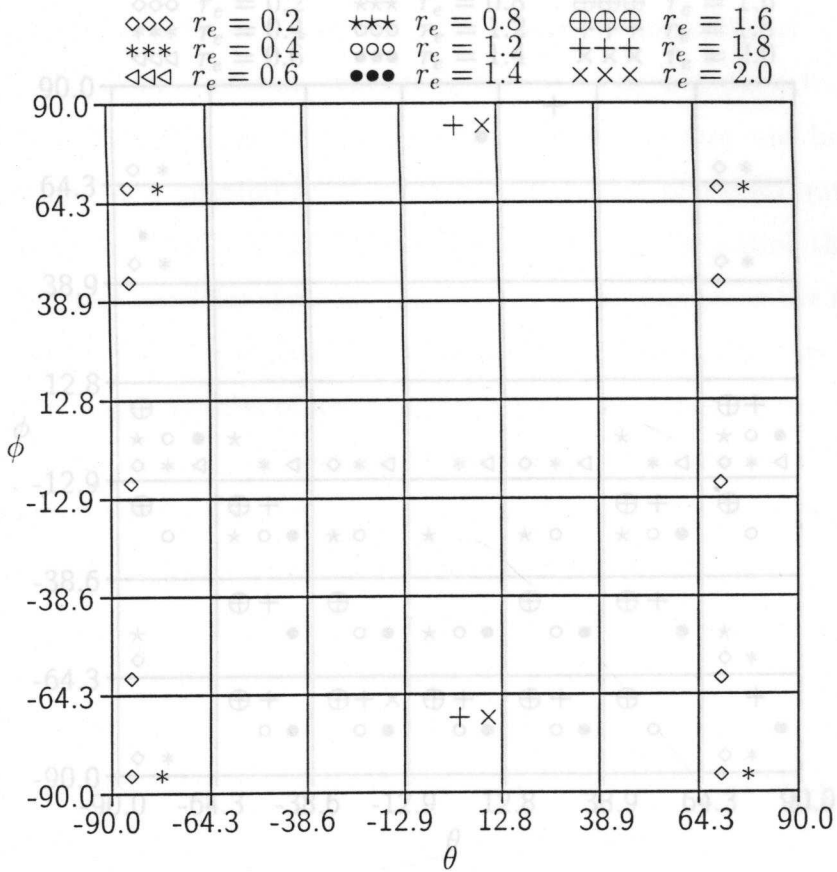


Table 3.1: Distribution of the evolution of initially uniformly distributed particles of different aspect ratios for the case $k_2 = 0$, $\omega = 0$, $5 \leq l_1 \leq 49$ and $10 \leq l_2 \leq 500$, where l_1 is the total number of particles in the grid on the average and l_2 is the total number of occurrences of the grid.

the particles can separate particles of aspect ratio 0.8 alone. However in this case, a constant force is preferable to a periodic force, since such particles are spread over a large number of grids in the case of a periodic force.

Further analysis of the tables indicate that the considered forces are not preferable for separating particles of aspect ratio 1.2 alone. A similar analysis shows that for particles of aspect ratio 1.2, a periodic force is preferable to separate particles of aspect ratio 1.2 alone. However, particles of aspect ratio greater than or equal to 1.6 individual separation may not be possible. However, a combination of separating particles of aspect ratio 1.8 by applying a periodic force of magnitude $k_2 = 0$, with the limitation that the occurrence of these particles alone are sensitive to small changes in the magnitude of the periodic force, for particles of higher aspect ratio particles appear in combination with particles of lower aspect ratio in all cases. If particles of lower aspect ratio are separated from the mixture, then particles of higher aspect ratio are separated from the mixture. In general, periodic forces are preferable to constant forces and also for separating particles of aspect ratio $r_e > 1$ however, for particles of aspect ratio $r_e \geq 1.6$ individual separation is not possible.

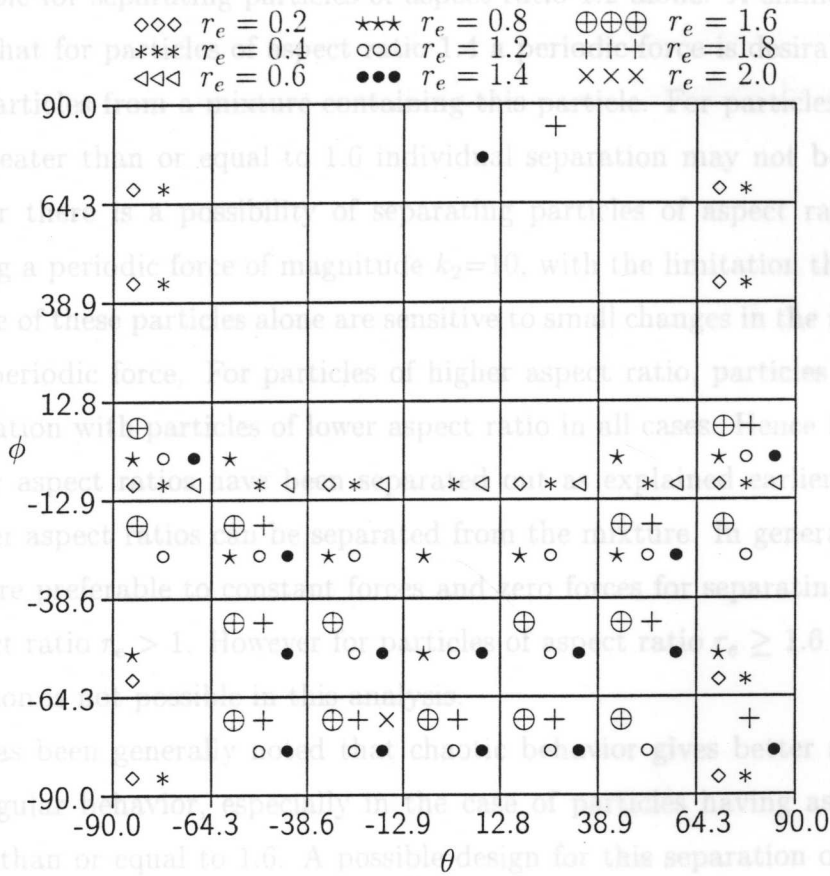


Table 3.2: Distribution of the evolution of initially uniformly distributed particles of different aspect ratios for the case $k_2 = 10.0$, $\omega = J = 2\pi(r_e + r_e^{-1})$, $5 \leq l_1 \leq 49$ and $10 \leq l_2 \leq 500$, where l_1 is the total number of particles in the grid on the average and l_2 is the total number of occurrences of the grid.

We believe that there is both important new physics and the possibility of new technology in such separations, since they could lead to better characterization of real suspensions for a study of their physical properties. This work also demonstrates the existence of chaotic parametric regimes in the problem

the particles can separate particles of aspect ratio 0.8 alone. However in this case, a constant force is preferable to a periodic force, since such particles are spread over a large number of grids in the case of a periodic force.

Further analysis of the tables indicate that the considered forces are not preferable for separating particles of aspect ratio 1.2 alone. A similar analysis shows that for particles of aspect ratio 1.4 a periodic force is desirable to separate particles from a mixture containing this particle. For particles of aspect ratio greater than or equal to 1.6 individual separation may not be possible. However there is a possibility of separating particles of aspect ratio 1.8 by applying a periodic force of magnitude $k_2=10$, with the limitation that the occurrence of these particles alone are sensitive to small changes in the magnitude of the periodic force. For particles of higher aspect ratio, particles appear in combination with particles of lower aspect ratio in all cases. Hence if particles of lower aspect ratios have been separated out as explained earlier, particles of higher aspect ratios can be separated from the mixture. In general periodic forces are preferable to constant forces and zero forces for separating particles of aspect ratio $r_e > 1$. However for particles of aspect ratio $r_e \geq 1.6$ individual separation is not possible in this analysis.

It has been generally noted that chaotic behavior gives better separation than regular behavior, especially in the case of particles having aspect ratio greater than or equal to 1.6. A possible design for this separation of particles with different aspect ratios based on the differences in the orientation of the particle may consist of a base plate having grooves along different orientations so that when the particles are oriented in such directions, they settle in a particular groove and can be separated out.

We believe that there is both important new physics and the possibility of new technology in such separations, since they could lead to better characterization of real suspensions for a study of their physical properties. This work also demonstrates the existence of chaotic parametric regimes in the problem

considered. This result may have considerable impact on the analysis of the practical applications referred to in the introduction. None of the authors dealing with the practical application of this problem have considered the existence of chaotic parametric regimes in their work.

One paper resulting from this work has been published in **Rheol. Acta** (1995), Germany. This paper has also been Listed in the Current World Literature section of **Current Opinion in Colloid and Interface Science** 1/4, 1996.

4.1 Introduction

After the discovery of chaos there arise lots of questions regarding the routes to the development of chaotic behaviour. What is the scenario behind the transition from regular behaviour to the chaotic behaviour as the control parameter is varied? Are there any universal patterns or sequences for this transition? Different routes to chaos have been reported in the chaos literature. The period doubling route to chaos, quasi-periodic route to chaos, intermittency route to chaos, crisis induced intermittency route to chaos etc. are some of the widely accepted scenarios. These routes to chaos are the ways in which the laminar flow loses stability and becomes chaotic. Manneville and Pomeau (1979) introduced the intermittency route to chaos in the Lorenz equations. The so-called intermittency occurs when nearly regular behaviour (laminar flow) is intermittently interrupted by chaotic excursions (bursts) at irregular intervals. As the control parameter α increases (and decreases), the strength of the chaotic burst also increases and finally the system ends up in fully chaotic behaviour. One of the routes to chaos is the class I intermittency route to chaos.